



# Structures and energetics of $\text{SiGeH}_z^{0,+1}$ , $\text{Ge}_2\text{H}_z^{0,+1}$ , and $\text{Si}_2\text{H}_z^{0,+1}$ : A systematic theoretical study

Liming Wang<sup>a,\*</sup>, Jingsong Zhang<sup>b</sup>

<sup>a</sup> School of Chemistry and Chemical Engineering, South China University of Technology, Guangzhou 510640, China

<sup>b</sup> Department of Chemistry and Air Pollution Research Center, University of California, Riverside, CA 92521, USA

## ARTICLE INFO

### Article history:

Received 8 September 2011

Received in revised form 9 December 2011

Accepted 9 December 2011

Available online 19 December 2011

### Keywords:

Silicon–germanium hydride

Germanium hydride

Silicon hydride

Appearance energy

Ionization energy

## ABSTRACT

The structural and energetic information of  $\text{Si}_x\text{Ge}_y\text{H}_z$  and ions is crucial in understanding the deposition processes in producing  $\text{Si}_x\text{Ge}_{1-x}$  semiconductor materials. This work presents theoretical studies on the structures and energetics of the simplest SiGe-hydrides and cations,  $\text{SiGeH}_z^{0,+1}$ , as well as  $\text{Ge}_2\text{H}_z^{0,+1}$  and  $\text{Si}_2\text{H}_z^{0,+1}$  for comparison. The structures are obtained at DFT-B3LYP and MP2 levels with 6-31+G(2df,p) basis set, and the electronic energies at Gaussian-4 (G4) level. The G4 energies are used to calculate the relative energies, bond dissociation energies, the adiabatic ionization energies ( $\text{IE}_a$ s) of neutral species, and the appearance energies (AEs) of cation fragments from  $\text{SiGeH}_6$ ,  $\text{Ge}_2\text{H}_6$ , and  $\text{Si}_2\text{H}_6$ . The relative energies and  $\text{IE}_a$ s for  $\text{Si}_2\text{H}_z$  and the total atomization energies of  $\text{Si}_2\text{H}_z$  and  $\text{Ge}_2\text{H}_z$  are compared and are in close agreement with previous theoretical and experimental studies, while the agreements on the AEs of  $\text{Si}_2\text{H}_z^+$  from  $\text{Si}_2\text{H}_6$  are less pronounced. The calculations suggest that the kinetic shift effect and potential barriers should be taken into account when using AEs for thermodynamic information of  $\text{Si}_2\text{H}_z^+$ ,  $\text{Ge}_2\text{H}_z^+$  and  $\text{SiGeH}_z^+$ .

© 2011 Elsevier B.V. All rights reserved.

## 1. Introduction

Silicon–germanium alloys,  $\text{Si}_x\text{Ge}_{1-x}$ , are of interest in micro-electronic industry, mainly because of the possibility of band-gap tuning and high-speed electronic devices based on the Si/ $\text{Si}_x\text{Ge}_{1-x}$  heterostructures [1]. The microcrystalline SiGe ( $\mu\text{c-SiGe}$ ) is also proposed as a substitute for thick  $\mu\text{c-Si}$  layer in solar cell systems to absorb sufficient light with thinner material and to allow more efficient use of longer wavelength light [2]. The main technique in growing the SiGe thin film is chemical vapor deposition (CVD), such as plasma-enhanced CVD (PECVD) from mixture of  $\text{SiH}_4$  or  $\text{Si}_2\text{H}_6$ ,  $\text{GeH}_4$ , and  $\text{H}_2$  [2–4], UV-laser assisted CVD (LCVD) [5], reactive thermal CVD from mixture of  $\text{Si}_2\text{H}_6$  and  $\text{GeF}_4$  over heated substrates [6], low-pressure CVD over heated quartz tube, and gas-source molecular beam epitaxy using  $\text{Si}_2\text{H}_6$  and  $\text{GeH}_4$  [7] or  $\text{H}_3\text{SiGeH}_3$  and  $\text{Ge}(\text{SiH}_3)_4$  [8]. In PECVD and LCVD, the precursors are fragmented in the gas phase to produce large amount of free radicals [9], including the silicon hydrides ( $\text{Si}_x\text{H}_z$ ), germanium hydrides ( $\text{Ge}_y\text{H}_z$ ), and hybrid silicon–germanium hydrides ( $\text{Si}_x\text{Ge}_y\text{H}_z$ ), and their cations in PECVD. The gas-phase thermodynamic properties, structures, and energetics of these hydrides and their cations would be helpful in understanding the PECVD and LCVD processes.

There have been a wealth of studies on the structures and energetics of  $\text{Si}_x\text{H}_z$  and  $\text{Ge}_y\text{H}_z$  hydrides, while the knowledge on hybrid  $\text{Si}_x\text{Ge}_y\text{H}_z$  hydrides is considerably scarce. Experimental studies on  $\text{Si}_x\text{Ge}_y\text{H}_z$  were limited to the enthalpy of formation of  $\text{SiGeH}_6$  [10,11], the atomization energies of SiGe [12,13] and  $\text{Si}_2\text{Ge}$ ,  $\text{SiGe}_2$  and  $\text{Si}_2\text{Ge}_2$  [13]. However, the obtained  $\Delta_f H^\circ(\text{SiGeH}_6)$  differed by as much as 85 kJ/mol. Theoretical studies on the thermodynamic properties of SiGe hydrides are also limited to SiGe [14–17] and propane-/butane-like hydrides [18], in contrast to the systematic studies on silicon hydrides [19–24] and germanium hydrides [25]. Theoretical studies on  $\text{SiGeH}_2$  and  $\text{SiGeH}_4$  [26–31] have focused on the non-classical structures similar to those found for  $\text{Si}_2\text{H}_z$  [32–36] and  $\text{Ge}_2\text{H}_z$  [34–42]. Here, we present a systematic theoretical study on the structures and energetics of  $\text{SiGeH}_z^{0,+1}$ ,  $\text{Si}_2\text{H}_z^{0,+1}$ , and  $\text{Ge}_2\text{H}_z^{0,+1}$  ( $z=0-6$ ), focusing on the relative stability of the isomers, the adiabatic ionization energies, and the energetics for the dissociative photoionization processes from  $\text{SiGeH}_6$ ,  $\text{Si}_2\text{H}_6$ , and  $\text{Ge}_2\text{H}_6$ .

## 2. Computational details

All molecular orbital and density functional theory (DFT) calculations are carried out by using Gaussian 03 suite of programs [43]. The geometries are optimized at B3LYP and MP2 levels with basis set 6-31+G(2df,p), which was also used in recent G4(MP2)-6X model chemistry [44]. Zero-point energy (ZPE) corrections are

\* Corresponding author. Tel.: +86 20 87112900; fax: +86 20 87112906.  
E-mail address: [wanglm@scut.edu.cn](mailto:wanglm@scut.edu.cn) (L. Wang).

obtained from the B3LYP harmonic frequencies with scale factor of 0.9888, which is obtained by comparing the estimated and the experimental ZPEs for a set of molecules [45]. Total energies are refined at G4 level with the effective electron correlation of CCSD(T,Full)/G3LargeXP+HFlimit [46]. The electronic energies of all species are given in Tables S1 (for isomers) and S2 (for transition states) of Supporting Information (SI).

### 3. Results and discussion

#### 3.1. Structures and energetics

Because of the capability of forming non-classical bonds between H and Si/Ge, multiple structures are possible for  $\text{Si}_2\text{H}_z^{0,+1}$ ,  $\text{Ge}_2\text{H}_z^{0,+1}$ , and  $\text{SiGeH}_z^{0,+1}$  ( $z=1-6$ ). The miscellaneous structures for  $\text{Si}_2\text{H}_z^{0,+1}$  from previous studies [32–36] are systematically examined here; while the structures of  $\text{Ge}_2\text{H}_z^{0,+1}$  and  $\text{SiGeH}_z^{0,+1}$  is searched by replacing Si with Ge-atom to the  $\text{Si}_2\text{H}_z^{0,+1}$  structures. The geometries of the most stable isomers of  $\text{Si}_2\text{H}_z^{0,+1}$ ,  $\text{Ge}_2\text{H}_z^{0,+1}$ , and  $\text{SiGeH}_z^{0,+1}$  are shown in Fig. 1 and others in SI (Figs. S1–S5).

The geometries are optimized at B3LYP and MP2 levels with 6-31+G(2df,p) basis sets. The geometries from B3LYP and MP2 agree with each other, while B3LYP predicts slightly longer bond lengths than MP2 for most of the cases, e.g. the B3LYP  $r(\text{Si}-\text{Ge})$  in  $\text{SiGeH}_6$  is 2.391 Å, being longer than the MP2 value of 2.370 Å and the experimental value of 2.364 Å [47]. Yet the energy differences between the B3LYP and MP2 geometries are rather small, being usually within 2 kJ/mol at G4 level, e.g. 0.8, 0.5, and 1.0 kJ/mol for  $\text{SiGeH}_6$ ,  $\text{Si}_2\text{H}_6$ , and  $\text{Ge}_2\text{H}_6$ , respectively (Table S1). For neutral hydrides, differences larger than 2 kJ/mol are found for  $\text{H}_2\text{Si}=\text{SiH}$ ,  $\text{H}_2\text{Ge}=\text{SiH}$ , and  $\text{Si}(\text{H})\text{Ge}$  ( $^2A'$ ), due to the large structure difference between B3LYP and MP2. For  $\text{H}_2\text{SiSiH}$  and  $\text{H}_2\text{GeSiH}$ , B3LYP predicts non-planar while MP2 predicts planar structures, with the MP2 structures being lower in energy by 5.0 and 5.7 kJ/mol. Further geometry refinement at QCISD/6-31+G(2df,p) level confirms the planar structures for  $\text{H}_2\text{SiSiH}$  and  $\text{H}_2\text{GeSiH}$ . Previous CCSD(T)/cc-pVTZ calculation also predicted a planar structure for  $\text{H}_2\text{SiSiH}$  [32]. For these three species, the G4 energy differences are less than 0.2 kJ/mol between QCISD and MP2 structures. Therefore, G4//MP2 energies will be adopted in the following discussion.

The G4//MP2 energies are used to calculate the relative energetics for various processes including ionization, dissociation, dissociative ionization, and reactions between  $\text{SiGeH}_z^{0,+1}$ ,  $\text{Si}_2\text{H}_z^{0,+1}$ , and  $\text{Ge}_2\text{H}_z^{0,+1}$ . The adiabatic ionization energies ( $\text{IE}_a$ ) for the most stable isomers are listed in Table 1, and the appearance energies (AE) of cation fragments in Table 2, while the complete dataset in Tables S3–S6, along with the previous theoretical and experimental values.

#### 3.2. $\text{Si}_2\text{H}_z^{0,+1}$

For  $\text{Si}_2\text{H}_z$ , current G4  $\text{IE}_a$ s and AEs agree excellently with the previous G2 predictions [21] within 0.04 eV, except that the G4  $\text{IE}_a$ s for  $\text{H}_2\text{SiSiH}$  and  $\text{H}_3\text{SiSi}$  are higher than the G2 ones by 0.08–0.17 eV. For  $\text{H}_2\text{SiSiH}$ , this is because that MP2(Full)/6-31G(d) in G2 predicted a non-planar structure while current MP2/6-31+G(2df,p) predicts a planar one. For  $\text{H}_3\text{SiSi}$ , the post-HF calculations in previous G2 suffered from strong spin contamination with  $\langle S^2 \rangle \sim 0.95$ , while the spin contamination in current G4 is negligible with  $\langle S^2 \rangle \sim 0.76$ . Therefore, the G2 electronic energies for  $\text{H}_2\text{SiSiH}$  and  $\text{H}_3\text{SiSi}$  were over-estimated due to incorrect structure and spin contamination, respectively, leading to the underestimated adiabatic IE.

Current G4 total atomization energies (TAEs) also agree excellently with the recent high-level CCSD(T)-DKH/CBS calculations for  $\text{Si}_2\text{H}_2$  and  $\text{Si}_2\text{H}_4$  within 4 kJ/mol [48,49], and with the early G2

predictions [21] within 6 kJ/mol for all the species except for  $\text{Si}_2$  and  $\text{H}_2\text{SiSiH}$ . For  $\text{H}_2\text{SiSiH}$ , the G2 TAE is lower than current G4//MP2 value by  $\sim 11$  kJ/mol, again due to fact that MP2(Full)/6-31G(d) in G2 predicted a non-planar structure.

A disagreement is found on the relative stability of  $\text{H}_3\text{SiSi}$  between current G4 and previous approximate CCSDT/cc-pVTZ ( $E_{\text{CCSDT/cc-pVTZ}} \approx E_{\text{CCSD(T)/cc-pVTZ}} + \Delta E_T$  with  $\Delta E_T = E_{\text{CCSDT/cc-pVDZ}} - E_{\text{CCSD(T)/cc-pVDZ}}$ ) calculations by Sari et al. [32], who located five structures for  $\text{Si}_2\text{H}_3$  as  $\text{H}_2\text{Si}(\text{H})\text{Si}$ ,  $\text{H}_2\text{SiSiH}$ ,  $\text{H}_3\text{SiSi}$ , and two  $\text{HSi}(\text{H})\text{SiH}$  isomers ( $C_2$  and  $C_1$ ) with relative energies of 0.0, 0.96, 13.2, 17.6, and 46.0 kJ/mol. The relative G4 energies are 0.0, 0.8, 2.4, 17.2, and 47.8 kJ/mol. At G4 level, the energy of  $\text{H}_3\text{SiSi}$  is close to those of  $\text{H}_2\text{Si}(\text{H})\text{Si}$  and  $\text{H}_2\text{SiSiH}$ , agreeing with the earlier theoretical predictions (MRCI, G2, and CCSD(T)) [20,21,50] but being contradictory to the CCSDT/cc-pVTZ prediction. The discrepancy on  $\text{H}_3\text{SiSi}$  is probably due to the unreasonably large  $\Delta E_T$  of 8.8 kJ/mol for  $\text{H}_3\text{SiSi}$  by Sari et al., if compared to  $\Delta E_T$  of less than 0.6 kJ/mol for other isomers in the calculations. We have re-examined and found  $\Delta E_T$  of 0.3 kJ/mol for  $\text{H}_3\text{SiSi}$  using NWChem 4.7 [51], and the unreasonably large  $\Delta E_T$  for  $\text{H}_3\text{SiSi}$  by Sari et al. may be a mistake. On the other hand, only  $\text{H}_2\text{SiSiH}$  has been observed and identified experimentally from microwave and infrared spectroscopy studies [32,50].

Ruscic and Berkowitz [52,53] have measured the  $\text{IE}_a$ s of  $\text{Si}_2\text{H}_z$  ( $z=2-6$ ) using photoionization mass spectrometry method, where  $\text{Si}_2\text{H}_z$  ( $z=2-5$ ) were generated by reacting  $\text{Si}_2\text{H}_6$  with F-atom. The observed  $\text{IE}_a$ s of  $8.09 \pm 0.03$ ,  $7.60 \pm 0.05$ , and  $9.74 \pm 0.02$  eV for  $z=4$ , 5, and 6 are supported by G4 predictions of 8.138 (for  $\text{H}_2\text{SiSiH}_2$ ), 7.709, and 9.656 eV, respectively; while the observed value of  $\leq 7.59$  eV for  $\text{Si}_2\text{H}_3$  cannot be certainly assigned to ionizations of  $\text{H}_2\text{SiSiH}$ ,  $\text{H}_2\text{Si}(\text{H})\text{Si}$ , or  $\text{H}_3\text{SiSi}$ . Ruscic and Berkowitz have assigned the observation to ionization  $[\text{H}_3\text{SiSi}]^+ \leftarrow \text{H}_3\text{SiSi}$  according to the G2  $\text{IE}_a(\text{H}_3\text{SiSi})$  of 7.57 eV [21], which is however much lower than G4 prediction of 7.691 eV as mentioned above. Current G4 calculations suggest that the observed  $\text{IE}_a(\text{Si}_2\text{H}_3)$  arise more likely from the ionization from  $[\text{H}_2\text{Si}(\text{H})\text{H}]^+ \leftarrow \text{H}_2\text{Si}(\text{H})\text{H}$  (7.579 eV by G4) or  $[\text{H}_2\text{Si}(\text{H})\text{Si}]^+ \leftarrow \text{H}_3\text{SiSi}$  (7.563 eV by G4) (Table S3). The observed  $\text{IE}_a(\text{Si}_2\text{H}_2)$  of  $8.20_{-0.01}^{+0.01}$  eV may arise from ionizations of  $\text{Si}(\text{H})_2\text{Si}$  (8.262 eV by G4) or  $\text{HSi}(\text{H})\text{Si}$  (8.231 eV by G4), albeit  $\text{HSi}(\text{H})\text{Si}$  is much less stable than  $\text{Si}(\text{H})_2\text{Si}$  by  $\sim 38$  kJ/mol.

Ion-complex structures are found as  $\text{Si}_2\text{H}_{z-2}^+-\text{H}_2$  for  $\text{Si}_2\text{H}_z^+$  ( $z=4-6$ ) (Figs. S1–S5), where the  $\text{Si}_2\text{H}_z^+$  moiety can be  $[\text{H}_2\text{SiSi}]^+$  or  $[\text{HSiSiH}]^+$ ,  $\text{Si}_2\text{H}_3^+$  be  $[\text{H}_2\text{Si}(\text{H})\text{Si}]^+$  or  $[\text{H}_2\text{SiSiH}]^+$ , and  $\text{Si}_2\text{H}_4^+$  be  $[\text{H}_2\text{SiSiH}_2]^+$  or  $[\text{H}_3\text{SiSiH}]^+$ . These ion-complex structures are much higher in energy than their 'normal' or H-bridged structures, and may serve as intermediates in  $\text{H}_2$ -eliminations from  $\text{Si}_2\text{H}_z^+$  cations.

#### 3.3. $\text{SiGeH}_z^{0,+1}$ and $\text{Ge}_2\text{H}_z^{0,+1}$

Structures of  $\text{SiGeH}_z^{0,+1}$  and  $\text{Ge}_2\text{H}_z^{0,+1}$  are searched by replacing Si-atom in  $\text{Si}_2\text{H}_z^{0,+1}$  with Ge-atom. Generally, geometries and electronic structures of  $\text{SiGeH}_z^{0,+1}$  and  $\text{Ge}_2\text{H}_z^{0,+1}$  are similar to their  $\text{Si}_2\text{H}_z^{0,+1}$  counterparts (Figs. S1–S5). The G4  $\text{IE}_a$ s and AEs are listed in Tables 1 and 2 and S3–S5. For  $\text{Ge}_2\text{H}_2$ , the G4 total atomization energies agree with the previous CCSD(T)/CBS predictions with 7 kJ/mol [25]. Although there have been some previous studies on the structures and energetics of  $\text{SiGe}^{0,+1}$  and  $\text{Ge}_2^{0,+1}$  at various levels of theory [15–17,54,55], current work presents a systematic study on  $\text{SiGeH}_z^{0,+1}$  and  $\text{Ge}_2\text{H}_z^{0,+1}$ . It is not surprising to find that  $\text{IE}_a(\text{Si}_2\text{H}_2) > \text{IE}_a(\text{SiGeH}_2) > \text{IE}_a(\text{Ge}_2\text{H}_2)$  for similar structures.

Experimental studies on  $\text{Ge}_2\text{H}_2$  and  $\text{SiGeH}_2$  are rather scarce. A near threshold photoionization study [56] found  $\text{IE}_a(\text{Ge}_2)$  in the range of 7.58–7.76 eV, which is supported by current G4 prediction of 7.662 eV, while other theoretical studies have predicted high value of 7.89 eV at B3LYP/6-311+G(3df) level [57] or low value

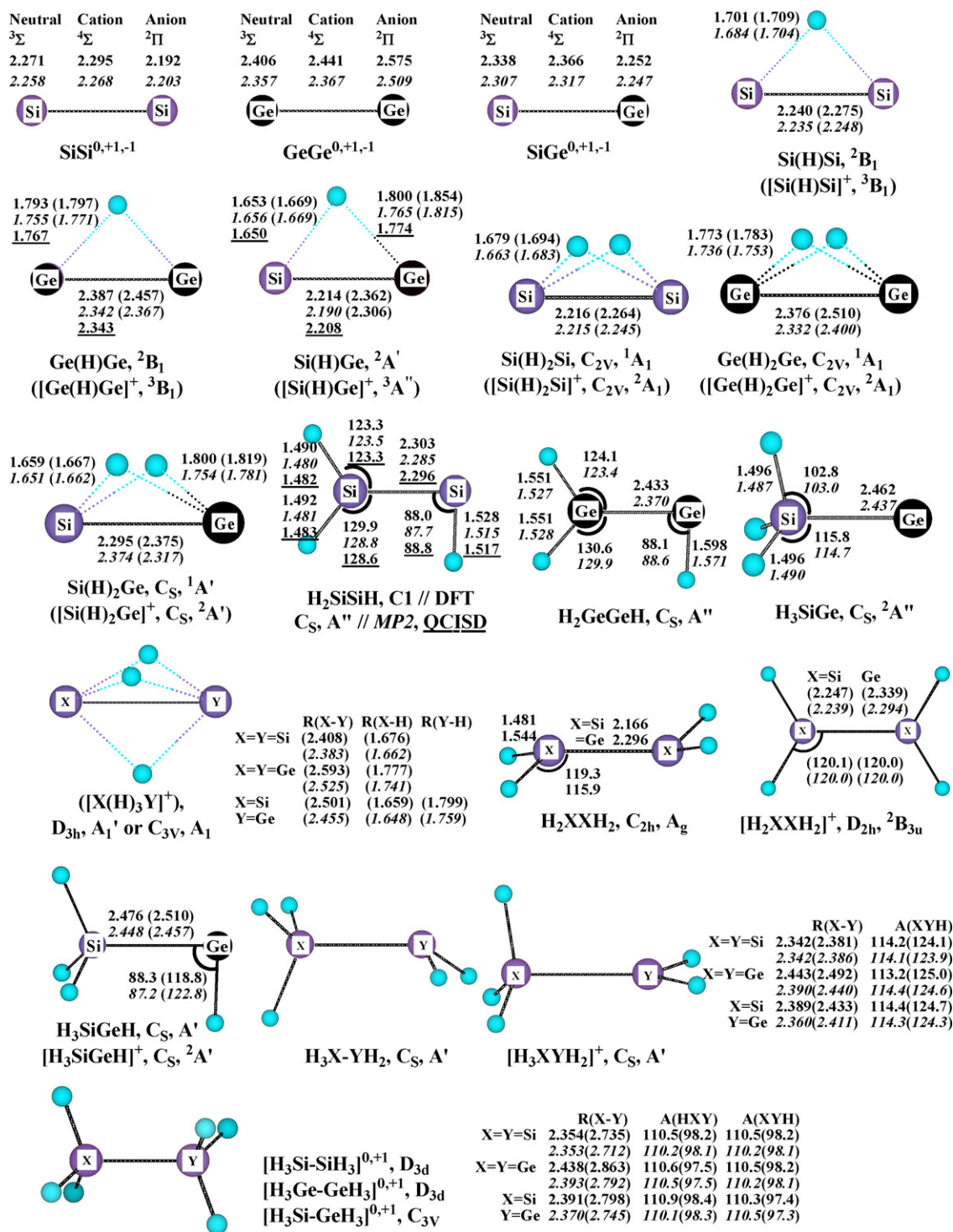


Fig. 1. The most stable structures for SiGeH<sub>2</sub><sup>0,+1</sup>, Ge<sub>2</sub>H<sub>2</sub><sup>0,+1</sup>, and Si<sub>2</sub>H<sub>2</sub><sup>0,+1</sup> at B3LYP, MP2 (in italics), and QCISD (with underline) levels of theory with 6-31+G(2df,p) basis sets. Parameters for cations are in round parenthesis.

of 7.45 eV at CCSD(T)/SDB-AVTZ level [17]. The G4 IE<sub>a</sub>(SiGe) of 7.785 eV is also much higher than MRCI/AVQZ value of 7.514 eV [54] and CCSD(T)/SDB-AVTZ value of 7.63 eV [17].

Bond dissociation energies ( $D_0$ ) of SiGe and Ge<sub>2</sub> have been measured experimentally.  $D_0(\text{Ge}_2) = 260.7 \pm 6.8$  kJ/mol has been obtained from the evaluation of more than 10 experimental measurements [58], and  $D_0(\text{SiGe})$  of  $297 \pm 21$  and  $292.7 \pm 8.6$  kJ/mol have been obtained from mass spectroscopic studies [12,13]. The experimental  $D_0(\text{Ge}_2)$  is supported by CCSD(T)/(SDB-AVTZ of

261.4 kJ/mol [17] and present G4 of 258.2 kJ/mol while being higher than previous G2 prediction of 246.9 kJ/mol [55]. For SiGe, present G4  $D_0$  of 284.7 kJ/mol ( $D_{298\text{K}}$  of 290.1 kJ/mol) is at the lower ends of both experimental uncertainty ranges, and also agrees with previous B3LYP prediction of 280 kJ/mol [15], CCSD(T)/(SDB-AVTZ of 278.5 kJ/mol [17], and MRCI/AVQZ of 280.2 kJ/mol [54], while all being much lower than another prediction of 304.9 kJ/mol at CCSD(T)/CBS level with core-valence and relativistic corrections [16].

**Table 1**Adiabatic ionization energies for the most stable Si<sub>2</sub>H<sub>z</sub>, Ge<sub>2</sub>H<sub>z</sub>, and SiGeH<sub>z</sub> isomers at G4 level (all in eV).

Processes	G4//DFT	G4//MP2	Lit. (Expt.)	Lit. (Theo.)
Si <sub>2</sub> ( <i>D</i> <sub>∞h</sub> , <sup>3</sup> Σ <sub>g</sub> ) → Si <sub>2</sub> <sup>+</sup> ( <i>D</i> <sub>∞h</sub> , <sup>4</sup> Σ <sub>g</sub> ) + e	7.924	7.921	7.921 <sup>a</sup>	7.82 <sup>d</sup> ; 7.913 <sup>e</sup> ; 7.94 <sup>f</sup>
Ge <sub>2</sub> ( <i>D</i> <sub>∞h</sub> , <sup>3</sup> Σ <sub>g</sub> ) → Ge <sub>2</sub> <sup>+</sup> ( <i>D</i> <sub>∞h</sub> , <sup>4</sup> Σ <sub>g</sub> ) + e	7.645	7.662	7.58–7.76 <sup>b</sup>	7.45 <sup>d</sup> ; 7.89 <sup>e</sup>
SiGe ( <i>C</i> <sub>∞v</sub> , <sup>3</sup> Σ) → SiGe <sup>+</sup> ( <i>C</i> <sub>∞v</sub> , <sup>4</sup> Σ) + e	7.785	7.785		
Si(H)Si ( <i>C</i> <sub>2v</sub> , <sup>2</sup> B <sub>1</sub> ) → [Si(H)Si] <sup>+</sup> ( <i>C</i> <sub>2v</sub> , <sup>3</sup> B <sub>1</sub> ) + e	8.112	8.109		8.10 <sup>f</sup>
Ge(H)Ge ( <i>C</i> <sub>2v</sub> , <sup>2</sup> B <sub>1</sub> ) → [Ge(H)Ge] <sup>+</sup> ( <i>C</i> <sub>2v</sub> , <sup>3</sup> B <sub>1</sub> ) + e	7.839	7.836		
Si(H)Ge ( <i>C</i> <sub>s</sub> , <sup>2</sup> A') → [Si(H)Ge] <sup>+</sup> ( <i>C</i> <sub>s</sub> , <sup>3</sup> A') + e	7.969	7.969		
Si(H) <sub>2</sub> Si ( <i>C</i> <sub>2v</sub> , A <sub>1</sub> ) → [Si(H) <sub>2</sub> Si] <sup>+</sup> ( <i>C</i> <sub>2v</sub> , <sup>2</sup> A <sub>1</sub> ) + e	8.263	8.262	8.20 <sup>+0.01</sup> <sub>-0.02</sub> <sup>c</sup>	8.30 <sup>f</sup>
Ge(H) <sub>2</sub> Ge ( <i>C</i> <sub>2v</sub> , A <sub>1</sub> ) → [Ge(H) <sub>2</sub> Ge] <sup>+</sup> ( <i>C</i> <sub>2v</sub> , <sup>2</sup> A <sub>1</sub> ) + e	7.972	7.967		
Si(H) <sub>2</sub> Ge ( <i>C</i> <sub>s</sub> , A') → [Si(H) <sub>2</sub> Ge] <sup>+</sup> ( <i>C</i> <sub>s</sub> , <sup>2</sup> A') + e	8.110	8.110		
H <sub>2</sub> SiSiH (C1//DFT)(C <sub>s</sub> //MP2) → [Si(H) <sub>3</sub> Si] <sup>+</sup> ( <i>D</i> <sub>3h</sub> , A <sub>1</sub> )	6.994	7.039		6.92 <sup>f</sup>
H <sub>2</sub> GeGeH ( <i>C</i> <sub>s</sub> , <sup>2</sup> A'') → [Ge(H) <sub>3</sub> Ge] <sup>+</sup> ( <i>D</i> <sub>3h</sub> , A <sub>1</sub> )	6.790	6.796		
H <sub>3</sub> SiGe ( <i>C</i> <sub>s</sub> , <sup>2</sup> A'') → [Si(H) <sub>3</sub> Ge] <sup>+</sup> ( <i>C</i> <sub>3v</sub> , A <sub>1</sub> )	7.306	7.302		
H <sub>2</sub> SiSiH <sub>2</sub> ( <i>C</i> <sub>2h</sub> , A <sub>g</sub> ) → [H <sub>2</sub> SiSiH <sub>2</sub> ] <sup>+</sup> ( <i>D</i> <sub>2h</sub> , <sup>2</sup> B <sub>3u</sub> ) + e	8.151	8.138	8.09 ± 0.03 <sup>c</sup>	8.11 <sup>f</sup>
H <sub>2</sub> GeGeH <sub>2</sub> ( <i>C</i> <sub>2h</sub> , A <sub>g</sub> ) → [H <sub>2</sub> GeGeH <sub>2</sub> ] <sup>+</sup> ( <i>D</i> <sub>2h</sub> , <sup>2</sup> B <sub>3u</sub> ) + e	8.096	8.083		
H <sub>3</sub> SiGeH ( <i>C</i> <sub>s</sub> , A') → [H <sub>3</sub> SiGeH] <sup>+</sup> ( <i>C</i> <sub>s</sub> , <sup>2</sup> A') + e	8.346	8.346		
H <sub>3</sub> SiSiH <sub>2</sub> ( <i>C</i> <sub>s</sub> , <sup>2</sup> A') → [H <sub>3</sub> SiSiH <sub>2</sub> ] <sup>+</sup> ( <i>C</i> <sub>s</sub> , A') + e	7.708	7.709	7.60 ± 0.05 <sup>c</sup>	7.64 <sup>f</sup>
H <sub>3</sub> GeGeH <sub>2</sub> ( <i>C</i> <sub>s</sub> , <sup>2</sup> A') → [H <sub>3</sub> GeGeH <sub>2</sub> ] <sup>+</sup> ( <i>C</i> <sub>s</sub> , A') + e	7.549	7.552		
H <sub>3</sub> SiGeH <sub>2</sub> ( <i>C</i> <sub>s</sub> , <sup>2</sup> A') → [H <sub>3</sub> SiGeH <sub>2</sub> ] <sup>+</sup> ( <i>C</i> <sub>s</sub> , A') + e	7.592	7.595		
H <sub>3</sub> SiSiH <sub>3</sub> ( <i>D</i> <sub>3d</sub> , A <sub>1g</sub> ) → [H <sub>3</sub> Si-SiH <sub>3</sub> ] <sup>+</sup> ( <i>D</i> <sub>3d</sub> , <sup>2</sup> A <sub>1g</sub> ) + e	9.659	9.656	9.74 ± 0.02 <sup>c</sup>	9.70 <sup>f</sup>
H <sub>3</sub> GeGeH <sub>3</sub> ( <i>D</i> <sub>3d</sub> , A <sub>1g</sub> ) → [H <sub>3</sub> Ge-GeH <sub>3</sub> ] <sup>+</sup> ( <i>D</i> <sub>3d</sub> , <sup>2</sup> A <sub>1g</sub> ) + e	9.424	9.419		
H <sub>3</sub> SiGeH <sub>3</sub> ( <i>C</i> <sub>3v</sub> , A <sub>1</sub> ) → [H <sub>3</sub> Si-GeH <sub>3</sub> ] <sup>+</sup> ( <i>C</i> <sub>3v</sub> , <sup>2</sup> A <sub>1</sub> ) + e	9.546	9.543		

<sup>a</sup> From mass-selected mass spectrometry [61].<sup>b</sup> Near threshold photoionization [56].<sup>c</sup> Photoionization mass spectrometry (values in parenthesis are the probable value) [52,53].<sup>d</sup> CCSD(T)/AVTZ [17].<sup>e</sup> CCSD(T)/CBS [62].<sup>f</sup> G2 [21].<sup>g</sup> B3LYP/6-311+G(3df) [57].**Table 2**Appearance energies of cation fragments from SiGeH<sub>6</sub>, Si<sub>2</sub>H<sub>4,5,6</sub>, and Ge<sub>2</sub>H<sub>6</sub> at G4 level (all in eV).

Processes	G4//DFT	G4//MP2	Lit. (Expt.) <sup>a</sup>	Lit. (Theo.) <sup>b</sup>
H <sub>2</sub> SiSiH <sub>2</sub> → [Si(H) <sub>2</sub> Si] <sup>+</sup> + H <sub>2</sub>	9.349	9.336	9.40	9.39
H <sub>2</sub> SiSiH <sub>2</sub> → [H <sub>2</sub> SiSi] <sup>+</sup> + H <sub>2</sub>	9.650	9.636	<9.62	
H <sub>2</sub> SiSiH <sub>2</sub> → [HSi(H)Si] <sup>+</sup> + H <sub>2</sub>	9.709	9.697		
H <sub>3</sub> SiSiH <sub>2</sub> → [Si(H) <sub>3</sub> Si] <sup>+</sup> + H <sub>2</sub> + e	8.732	8.729	8.74 <sup>a</sup> ; ≤9.24	8.72
Si <sub>2</sub> H <sub>6</sub> → [H <sub>3</sub> SiSiH <sub>2</sub> ] <sup>+</sup> + H + e	11.491	11.492	≤11.59 ± 0.02	11.45
Si <sub>2</sub> H <sub>6</sub> → [H <sub>2</sub> Si(H)SiH <sub>2</sub> ] <sup>+</sup> + H + e	11.493	11.494		
Si <sub>2</sub> H <sub>6</sub> → [H <sub>2</sub> SiSiH <sub>2</sub> ] <sup>+</sup> + H <sub>2</sub> + e	10.134	10.133	≤10.04 ± 0.01	10.09
Si <sub>2</sub> H <sub>6</sub> → [H <sub>3</sub> SiSiH] <sup>+</sup> + H <sub>2</sub> + e	10.695	10.694	≤10.81 ± 0.02	10.68
Si <sub>2</sub> H <sub>6</sub> → [Si(H) <sub>3</sub> Si] <sup>+</sup> + H <sub>2</sub> + H + e	12.515	12.513	≤13.00 ± 0.04 (≤12.70)	12.54
Si <sub>2</sub> H <sub>6</sub> → [Si(H) <sub>2</sub> Si] <sup>+</sup> + H <sub>2</sub> + H <sub>2</sub> + e	11.332	11.331		11.36
Si <sub>2</sub> H <sub>6</sub> → [H <sub>2</sub> SiSi] <sup>+</sup> + H <sub>2</sub> + H <sub>2</sub> + e	11.632	11.631	≤11.72 <sup>+0.02</sup> <sub>-0.04</sub> (≤11.57 ± 0.02)	
Si <sub>2</sub> H <sub>6</sub> → [HSi(H)Si] <sup>+</sup> + H <sub>2</sub> + H <sub>2</sub> + e	11.691	11.692		
Si <sub>2</sub> H <sub>6</sub> → SiH <sub>3</sub> + SiH <sub>3</sub> <sup>+</sup> + e	11.427	11.425	≤11.72 ± 0.00	
Ge <sub>2</sub> H <sub>6</sub> → [H <sub>3</sub> GeGeH <sub>2</sub> ] <sup>+</sup> + H + e	11.070	11.070		
Ge <sub>2</sub> H <sub>6</sub> → [H <sub>2</sub> Ge(H)GeH <sub>2</sub> ] <sup>+</sup> + H + e	11.214	11.221		
Ge <sub>2</sub> H <sub>6</sub> → [H <sub>2</sub> GeGeH <sub>2</sub> ] <sup>+</sup> + H <sub>2</sub> + e	9.558	9.559		
Ge <sub>2</sub> H <sub>6</sub> → [H <sub>3</sub> GeGeH] <sup>+</sup> + H <sub>2</sub> + e	9.915	9.916		
Ge <sub>2</sub> H <sub>6</sub> → [Ge(H) <sub>3</sub> Ge] <sup>+</sup> + H <sub>2</sub> + H + e	11.334	11.343		
Ge <sub>2</sub> H <sub>6</sub> → [Ge(H) <sub>2</sub> Ge] <sup>+</sup> + H <sub>2</sub> + H <sub>2</sub> + e	9.912	9.918		
Ge <sub>2</sub> H <sub>6</sub> → GeH <sub>3</sub> + GeH <sub>3</sub> <sup>+</sup> + e	11.077	11.076		
SiGeH <sub>6</sub> → [H <sub>3</sub> SiGeH <sub>2</sub> ] <sup>+</sup> + H + e	11.094	11.094		
SiGeH <sub>6</sub> → [H <sub>3</sub> GeSiH <sub>2</sub> ] <sup>+</sup> + H + e	11.472	11.473		
SiGeH <sub>6</sub> → [H <sub>2</sub> SiGeH <sub>2</sub> ] <sup>+</sup> + H <sub>2</sub> + e	9.849	9.848		
SiGeH <sub>6</sub> → [H <sub>3</sub> SiGeH] <sup>+</sup> + H <sub>2</sub> + e	9.968	9.967		
SiGeH <sub>6</sub> → [Si(H) <sub>3</sub> Ge] <sup>+</sup> + H <sub>2</sub> + H	11.919	11.921		
SiGeH <sub>6</sub> → [Si(H) <sub>2</sub> Ge] <sup>+</sup> + H <sub>2</sub> + H <sub>2</sub>	10.620	10.625		
SiGeH <sub>6</sub> → SiH <sub>3</sub> + GeH <sub>3</sub> <sup>+</sup> + e	11.197	11.198		
SiGeH <sub>6</sub> → GeH <sub>3</sub> + SiH <sub>3</sub> <sup>+</sup> + e	11.306	11.305		

<sup>a</sup> Photoionization mass spectrometry (values in parenthesis are the probable value) [52,53].<sup>b</sup> G2 [21].

Because σ(Si–H) bonds are stronger than σ(Ge–H) bonds, certain H-bridged neutral and cation structures similar to Si<sub>2</sub>H<sub>z</sub><sup>0,+1</sup> cannot be located at B3LYP or MP2 level for SiGeH<sub>z</sub><sup>0,+1</sup> since they tend to form ‘normal’ σ(Si–H) bonds, e.g., optimizations of H<sub>2</sub>Si(H)GeH and [H<sub>2</sub>Si(H)GeH]<sup>+</sup> lead to H<sub>3</sub>SiGeH and [H<sub>3</sub>SiGeH]<sup>+</sup>. The relative stability of SiGeH<sub>z</sub><sup>0,+1</sup> is nearly in line with the

number of ‘normal’ σ(Si–H) bonds for z=3 to 5, i.e. the most stable SiGeH<sub>z</sub><sup>0,+1</sup> isomers are Si(H)Ge (<sup>2</sup>A'') and [Si(H)Ge]<sup>+</sup> (<sup>3</sup>A'') for z=1, Si(H)<sub>2</sub>Ge and [Si(H)<sub>2</sub>Ge]<sup>+</sup>–[H<sub>2</sub>SiGe]<sup>+</sup> for z=2, H<sub>3</sub>SiGe (<sup>2</sup>A'') and [Si(H)<sub>3</sub>Ge]<sup>+</sup> (*C*<sub>3v</sub>, A<sub>1</sub>) for z=3, H<sub>3</sub>SiGeH (*C*<sub>s</sub>, A') and [H<sub>2</sub>SiGeH<sub>2</sub>]<sup>+</sup> (*C*<sub>2v</sub>, <sup>2</sup>B<sub>1</sub>) for z=4, and H<sub>3</sub>SiGeH<sub>2</sub> and [H<sub>3</sub>SiGeH<sub>2</sub>]<sup>+</sup> for z=5.

Being similar to  $\text{Si}_2\text{H}_z^+$ , ion-complex structures are also found for  $\text{Ge}_2\text{H}_z^+$  and  $\text{SiGeH}_z^+$  ( $z=4-6$ ) as  $[\text{HGeGeH}]^+-\text{H}_2$ ,  $[\text{H}_2\text{GeGe}]^+-\text{H}_2$ ,  $[\text{H}_2\text{Ge}(\text{H})\text{Ge}]^+-\text{H}_2$ ,  $[\text{H}_3\text{GeGeH}]^+-\text{H}_2$ , and  $[\text{H}_2\text{GeGeH}_2]^+-\text{H}_2$  for  $\text{Ge}_2\text{H}_z^+$ , and as  $[\text{HSiGeH}]^+-\text{H}_2$ ,  $[\text{H}_2\text{SiGe}]^+-\text{H}_2$ ,  $[\text{H}_2\text{GeSi}]^+-\text{H}_2$ ,  $[\text{H}_2\text{Si}(\text{H})\text{Ge}]^+-\text{H}_2$ ,  $[\text{H}_2\text{GeSiH}]^+-\text{H}_2$ ,  $[\text{H}_3\text{SiGeH}]^+-\text{H}_2$ ,  $[\text{H}_3\text{GeSiH}]^+$ ,  $[\text{H}_2\text{SiGeH}_2]^+-\text{H}_2$ , and  $[\text{H}_2\text{GeSiH}_2]^+-\text{H}_2$  for  $\text{SiGeH}_z^+$ . These ion complexes are again at much higher energies than their 'normal' or H-bridged isomers (Table S1) and would serve as the intermediates in the  $\text{H}_2$ -elimination processes from  $\text{Ge}_2\text{H}_z^+$  and  $\text{SiGeH}_z^+$ .

### 3.4. Thermal neutrality

Gunn and Kindsvater [10] have obtained  $\Delta_r H^\circ_{298\text{K}}$  of  $-1.6\text{ kJ/mol}$  for reaction  $\text{Si}_2\text{H}_6 + \text{Ge}_2\text{H}_6 \rightarrow 2\text{H}_3\text{SiGeH}_3$  by comparing the heats of decomposition of  $\text{H}_3\text{SiGeH}_3$  and  $\text{Si}_2\text{H}_6\text{-Ge}_2\text{H}_6$  mixtures. The value is supported here by G4 value of  $-0.1\text{ kJ/mol}$ . The nearly thermal neutrality of this reaction can be extended to other  $\text{Si}_2\text{H}_z^{0,+1}$ ,  $\text{Ge}_2\text{H}_z^{0,+1}$ , and  $\text{SiGeH}_z^{0,+1}$ , e.g.

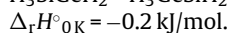
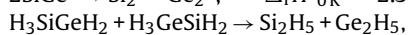
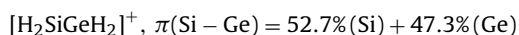
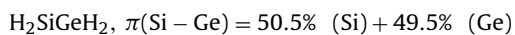
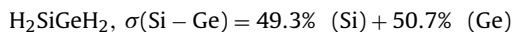
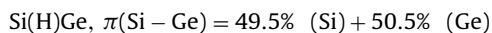
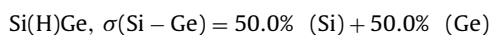


Table S6 lists the enthalpy changes and demonstrates the thermal neutrality for other reactions. The absolute enthalpy changes are all within  $4\text{ kJ/mol}$ , except for the two reactions of  $[\text{HSi}(\text{H})_2\text{GeH}]^+$  because the two bridged H-atoms bond preferentially to Si-atom in the cations. As a result of thermal neutrality for both neutral and cationic species,  $\text{IE}_a$  of  $\text{SiGeH}_z$  is about the average of the  $\text{IE}_a$ s of the corresponding  $\text{Si}_2\text{H}_z$  and  $\text{Ge}_2\text{H}_z$  (Table 1), e.g.  $\text{IE}_a(\text{SiGe})$  ( $7.785\text{ eV}$ )  $\sim (\text{IE}_a(\text{Si}_2) + \text{IE}_a(\text{Ge}_2))/2$  ( $7.782\text{ eV}$ ) by G4. Similar equality for  $\text{IE}_a$  can also be identified from previous CCSD(T)/(SDB-)AVTZ study with  $\text{IE}_a(\text{SiGe})$  ( $7.63\text{ eV}$ )  $\sim (\text{IE}_a(\text{Si}_2) + \text{IE}_a(\text{Ge}_2))/2$  ( $7.64\text{ eV}$ ) [17], albeit the differences on  $\text{IE}_a$ s between G4 and CCSD(T)/(SDB-)AVTZ are as large as  $0.15\text{ eV}$ . The validity of the thermal neutrality and equality in  $\text{IE}_a$  can provide a criterion for future experimental measurements on the thermodynamic properties and  $\text{IE}_a$ s of  $\text{Ge}_2\text{H}_z$  and  $\text{SiGeH}_z$ .

The thermal neutrality is rooted on the fact that Si and Ge contribute almost equally when they form  $\sigma$ - and  $\pi$ -bonds by using the NBO (natural bond order) analysis as embedded in Gaussian 03 [59]. For example, NBO analysis find the following orbital contributions in  $\text{Si}(\text{H})\text{Ge}$  and  $\text{H}_2\text{SiGeH}_2$ :



The almost equal contributions from Si and Ge in both neutral hydrides and cations warrants the approximate equality of  $\text{IE}_a(\text{SiGeH}_z) \sim [\text{IE}_a(\text{Si}_2\text{H}_z) + \text{IE}_a(\text{Ge}_2\text{H}_z)]/2$ .

### 3.5. Photoionization and ion fragmentation of $\text{SiGeH}_6$ , $\text{Si}_2\text{H}_6$ , and $\text{Ge}_2\text{H}_6$

One method to measure the bond dissociation energies and enthalpies of formation of free radicals is by photoionization mass spectrometry, measuring the  $\text{IE}_a$ s and AEs of ion fragments [60]. This has been used by Ruscic and Berkowitz to measure the enthalpies of formation of  $\text{Si}_2\text{H}_z$  radicals from the dissociative photoionization of  $\text{Si}_2\text{H}_6$  [52,53]. However, the determinations of  $\text{IE}_a$ s and AEs may suffer from the small Franck-Condon factor at

the ionization thresholds, thermal shift, and kinetic shift when a "tight" transition state exists for the dissociation channels, etc. The measured AEs may also correspond to the potential barrier when the transition state is at higher energy than the dissociation limit. For example, Ruscic and Berkowitz [52,53] assumed routes  $\text{Si}_2\text{H}_6^+ \rightarrow \text{Si}_2\text{H}_5^+ \rightarrow \text{Si}_2\text{H}_3^+$  for  $\text{Si}_2\text{H}_3^+$  and  $\text{Si}_2\text{H}_6^+ \rightarrow \text{Si}_2\text{H}_4^+ \rightarrow \text{Si}_2\text{H}_2^+$  for  $\text{Si}_2\text{H}_2^+$ . Transition states are expected for the  $\text{H}_2$ -elimination processes, and the barriers and kinetic shifts may affect the AE measurements for  $\text{Si}_2\text{H}_3^+$  and  $\text{Si}_2\text{H}_2^+$ . The potential energy surfaces (PESs) for decomposition and isomerization reactions of  $\text{Si}_2\text{H}_z^+$ ,  $\text{Ge}_2\text{H}_z^+$ , and  $\text{SiGeH}_z^+$  ( $z=4, 5, 6$ ) are explored here at G4 level. Transition states are searched and confirmed using Intrinsic Reaction Coordinate (IRC) method (Fig. 2 and Table S2). Present study attempts to interpret the experimental observations of  $\text{Si}_2\text{H}_z^+$  from  $\text{Si}_2\text{H}_6$ ,  $\text{Si}_2\text{H}_5$ , and  $\text{Si}_2\text{H}_4$  [52,53], and to predict the appearance of  $\text{Ge}_2\text{H}_z^+$  and  $\text{SiGeH}_z^+$  from  $\text{Ge}_2\text{H}_6$  and  $\text{SiGeH}_6$ , for which no previous experimental or theoretical study is available.

Fig. 3 shows the potential energy diagram of  $\text{Si}_2\text{H}_6^+$ . The predicted and measured AEs for  $\text{SiH}_3^+$  and  $\text{Si}_2\text{H}_z^+$  ( $z=2-5$ ) are in reasonable agreement with the experimental values (Table 2). For  $\text{Si}_2\text{H}_4^+$ , the appearance of  $[\text{H}_2\text{SiSiH}_2]^+$  from  $[\text{H}_3\text{SiSiH}_3]^+$  via  $[\text{H}_2\text{SiSiH}_2]^+-\text{H}_2$  has a high barrier which is above  $[\text{H}_2\text{SiSiH}_2]^+ + \text{H}_2$ , while the barrier from  $[\text{H}_3\text{SiSiH}_3]^+$  to  $[\text{H}_3\text{SiSiH}]^+$  is below  $[\text{H}_3\text{SiSiH}]^+ + \text{H}_2$  because of the existence of ion complex  $[\text{H}_3\text{SiSiH}]^+-\text{H}_2$ . Therefore, the appearance of  $[\text{H}_3\text{SiSiH}]^+$  arises likely from excitation to  $[\text{H}_3\text{SiSiH}_3]^+$ , followed by isomerization and decomposition, while the appearance of  $[\text{H}_2\text{SiSiH}_2]^+$  arises likely from the direct ionization to ion complex  $[\text{H}_2\text{SiSiH}_2]^+-\text{H}_2$  with very small Franck-Condon factor. This is consistent with the observation that the signal at the onset for  $[\text{H}_2\text{SiSiH}_2]^+$  is much weaker than that for  $[\text{H}_3\text{SiSiH}]^+$  in the photoionization study [53].

The appearances of  $\text{Si}_2\text{H}_3^+$  and  $\text{Si}_2\text{H}_2^+$  from  $\text{Si}_2\text{H}_6$  involve consecutive dissociation steps. From the photoionization study, Ruscic and Berkowitz [53] obtained  $\text{AE}(\text{Si}_2\text{H}_3^+/\text{Si}_2\text{H}_6)$  of  $\leq 13.00 \pm 0.04\text{ eV}$  (most probably  $12.70\text{ eV}$ ) and  $\text{AE}(\text{Si}_2\text{H}_2^+/\text{Si}_2\text{H}_6)$  of  $\leq 11.72^{+0.02}_{-0.04}\text{ eV}$  (most probably  $\leq 11.57 \pm 0.03\text{ eV}$ , and assumed  $\text{Si}_2\text{H}_3^+$  and  $\text{Si}_2\text{H}_2^+$  were from the decomposition of  $\text{Si}_2\text{H}_5^+$  and  $\text{Si}_2\text{H}_4^+$ , respectively. G4 finds the thermodynamic limits of  $13.061$ ,  $12.904$ , and  $12.513\text{ eV}$  for the appearances of  $[\text{H}_2\text{Si}(\text{H})\text{Si}]^+$ ,  $[\text{HSi}(\text{H})_2\text{Si}]^+$ , and  $[\text{Si}(\text{H})_3\text{Si}]^+$ , respectively, and the transition barriers from either  $\text{Si}_2\text{H}_5^+$  or  $\text{Si}_2\text{H}_4^+$  to  $\text{Si}_2\text{H}_3^+$  are all below the thermodynamic limits. Therefore, the observed  $\text{AE}(\text{Si}_2\text{H}_3^+/\text{Si}_2\text{H}_6)$  cannot be assigned determinately. Similarly, the G4 thermodynamic limits are  $11.331$ ,  $11.631$ , and  $11.692\text{ eV}$  for  $[\text{Si}(\text{H})_2\text{Si}]^+$ ,  $[\text{H}_2\text{SiSi}]^+$ , and  $[\text{HSi}(\text{H})\text{Si}]^+$ , respectively. The barrier from  $[\text{H}_3\text{SiSiH}]^+$  to  $[\text{H}_2\text{SiSi}]^+-\text{H}_2$  is slightly higher than  $[\text{H}_2\text{SiSi}]^+ + \text{H}_2$  ( $11.731\text{ eV}$ ), while the barrier from  $[\text{H}_3\text{SiSiH}]^+$  to  $[\text{HSi}(\text{H})\text{Si}]^+-\text{H}_2$  is much higher than the fragments ( $12.197\text{ eV}$ ). Therefore, the  $\text{Si}_2\text{H}_2^+$  observed might be  $[\text{H}_2\text{SiSi}]^+$  via  $[\text{H}_3\text{SiSiH}]^+$ .

Ruscic and Berkowitz [52,53] also observed  $\text{AE}(\text{Si}_2\text{H}_3^+/\text{Si}_2\text{H}_5)$  of  $\leq 9.24\text{ eV}$ ,  $\text{AE}(\text{Si}_2\text{H}_2^+/\text{Si}_2\text{H}_4)$  of  $\leq 9.62\text{ eV}$ , a weak tail with onset at  $\sim 8.74\text{ eV}$  for  $\text{Si}_2\text{H}_3^+/\text{Si}_2\text{H}_5$ , and a weak onset at  $9.40\text{ eV}$  for  $\text{Si}_2\text{H}_2^+/\text{Si}_2\text{H}_4$ . The observed  $\text{AE}(\text{Si}_2\text{H}_3^+)$  is supported by the G4 thermodynamic limit of  $9.247\text{ eV}$  for  $[\text{H}_2\text{Si}(\text{H})\text{Si}]^+ + \text{H}_2$ , while the weak tail at  $8.74\text{ eV}$  is likely for  $[\text{Si}(\text{H})_3\text{Si}]^+/\text{Si}_2\text{H}_5$  ( $\text{AE} = 8.729\text{ eV}$  by G4). Note that the barrier from  $[\text{H}_3\text{SiSiH}_2]^+$  to  $[\text{H}_2\text{SiSiH}]^+-\text{H}_2$  is below  $[\text{H}_2\text{Si}(\text{H})\text{Si}]^+ + \text{H}_2$ . The observed  $\text{AE}(\text{Si}_2\text{H}_2^+/\text{Si}_2\text{H}_4)$  is comparable to the G4 AEs of  $9.636$  and  $9.697\text{ eV}$  for  $[\text{H}_2\text{SiSi}]^+$  and  $[\text{HSi}(\text{H})\text{Si}]^+ + \text{H}_2$  from  $\text{H}_2\text{SiSiH}_2$ , albeit a transition state from  $[\text{H}_2\text{SiSiH}_2]^+$  to  $[\text{H}_2\text{SiSi}]^+$  exists at a slightly high position of  $9.741\text{ eV}$ , while the weak tail at  $9.40\text{ eV}$  is probably due to  $[\text{Si}(\text{H})_2\text{Si}]^+$  from  $\text{H}_2\text{SiSiH}_2$  ( $\text{AE} = 9.336\text{ eV}$  by G4) (Table 2).

No previous study is available on the dissociative photoionization of  $\text{Ge}_2\text{H}_6$  or  $\text{SiGeH}_6$ . The G4 relative energies and potential energy diagrams are present here for future reference (Tables S4 and S5 and Figs. S6 and S7). The potential energy diagram for  $\text{Ge}_2\text{H}_6^+$  indicates that the onsets for  $[\text{H}_2\text{GeGeH}_2]^+$  and

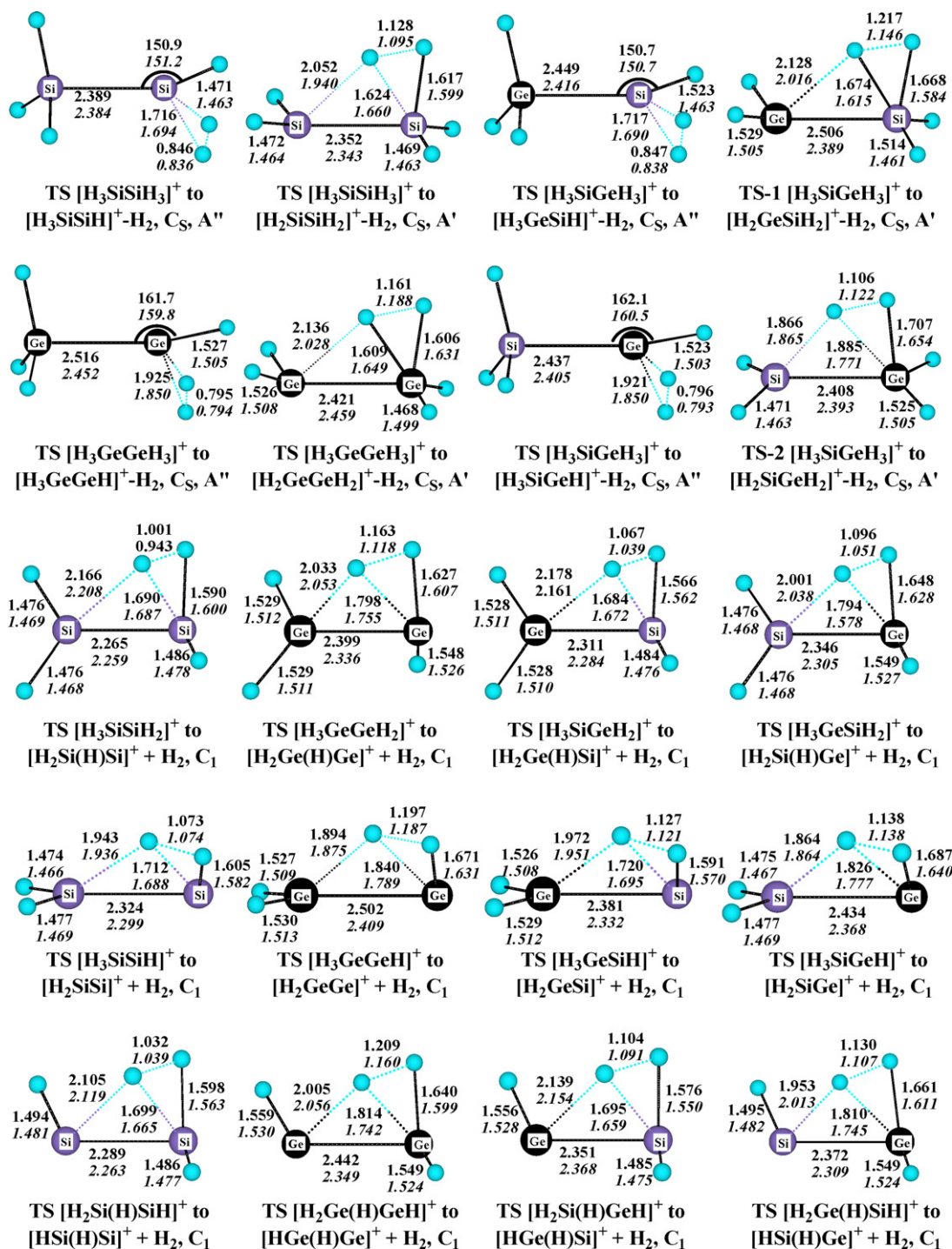


Fig. 2. Optimized geometries of transition states for H<sub>2</sub>-eliminations from Si<sub>2</sub>H<sub>2</sub><sup>+</sup>, Ge<sub>2</sub>H<sub>2</sub><sup>+</sup>, and SiGeH<sub>2</sub><sup>+</sup> (z=4–6) at levels of B3LYP and MP2 (in italics).

[H<sub>3</sub>GeGeH]<sup>+</sup> from Ge<sub>2</sub>H<sub>6</sub> would correspond to the weak photoionization to [H<sub>2</sub>GeGeH<sub>2</sub>]<sup>+</sup>-H<sub>2</sub> and [H<sub>3</sub>GeGeH]<sup>+</sup>-H<sub>2</sub>, respectively, because the transition barriers from the [H<sub>3</sub>Ge-GeH<sub>3</sub>]<sup>+</sup> to both complexes and fragments are higher than the exit limits. The most likely route for Ge<sub>2</sub>H<sub>3</sub><sup>+</sup> are Ge<sub>2</sub>H<sub>6</sub> → Ge<sub>2</sub>H<sub>4</sub><sup>+</sup> → Ge<sub>2</sub>H<sub>3</sub><sup>+</sup>, while the thermodynamic limits for Ge<sub>2</sub>H<sub>2</sub><sup>+</sup> would likely be over-estimated in the photoionization study because the transition barriers from [H<sub>3</sub>GeGeH]<sup>+</sup> to Ge<sub>2</sub>H<sub>2</sub><sup>+</sup> are higher than [H<sub>2</sub>GeGe]<sup>+</sup> and [HGe(H)Ge]<sup>+</sup> by 0.586 and 1.027 eV. Similarly, weak onsets are expected for [H<sub>2</sub>SiGeH<sub>2</sub>]<sup>+</sup> and [H<sub>3</sub>SiGeH]<sup>+</sup> from SiGeH<sub>6</sub> because of the high transition barriers and large structural changes to [H<sub>2</sub>SiGeH<sub>2</sub>]<sup>+</sup>-H<sub>2</sub>

and [H<sub>3</sub>SiGeH]<sup>+</sup>-H<sub>2</sub>, while appearance of [H<sub>3</sub>GeSiH]<sup>+</sup> is expected to be clear because the transition barrier from [H<sub>3</sub>SiGeH<sub>3</sub>]<sup>+</sup> to [H<sub>3</sub>GeSiH]<sup>+</sup>-H<sub>2</sub> is below the fragment [H<sub>3</sub>GeSiH]<sup>+</sup> + H<sub>2</sub>. Again the transition barrier from SiGeH<sub>4</sub><sup>+</sup> to [H<sub>2</sub>SiGe]<sup>+</sup>, [H<sub>2</sub>GeSi]<sup>+</sup>, [HSi(H)Ge]<sup>+</sup>, and [HGe(H)Si]<sup>+</sup> are above their thermodynamic limits by 0.469, 0.225, 0.774, and 0.770 eV, respectively, and their AEs might be overestimated.

Overall, the G4 results for the energetics of neutral Si<sub>2</sub>H<sub>n</sub> and Ge<sub>2</sub>H<sub>n</sub> are in close agreements with the previous G2 and various intensive CCSDT/CBS predictions. The G4 ionization energies of Si<sub>2</sub>H<sub>2</sub> and appearance energies of Si<sub>2</sub>H<sub>2</sub><sup>+</sup> from Si<sub>2</sub>H<sub>6</sub> were compared

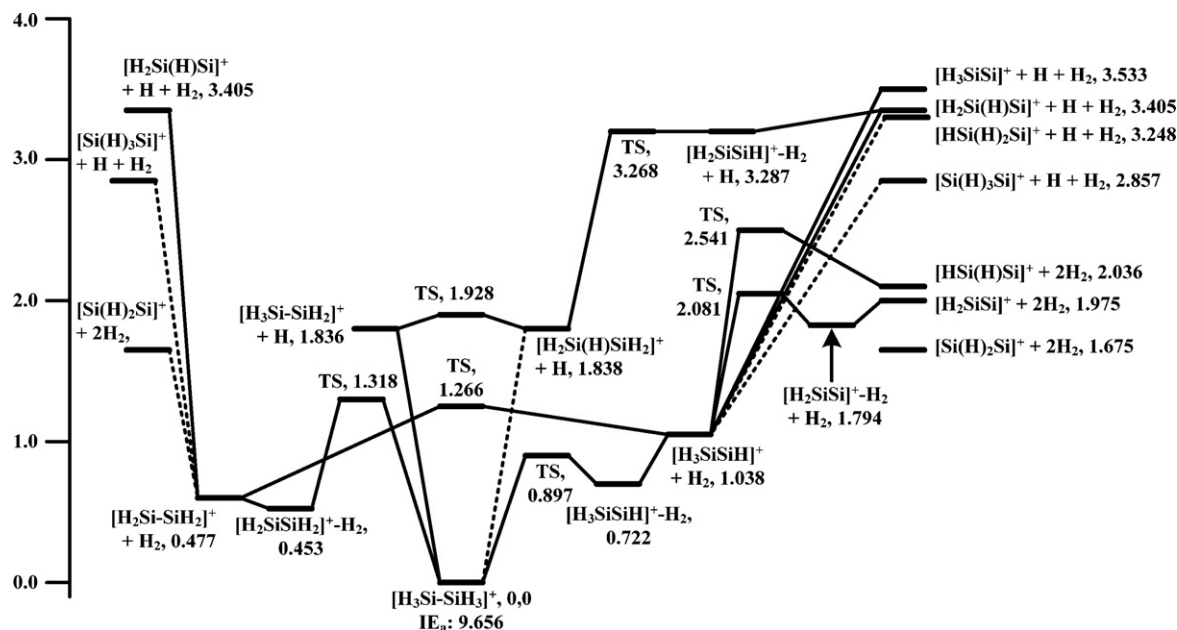


Fig. 3. The potential energy diagrams for  $\text{Si}_2\text{H}_6^+$  at G4//MP2 level (in eV).

with the experimental measurements by Ruscic and Berkowitz [52,53], of which the G4 IE<sub>s</sub> are in good agreement with the experimental values, while the agreements in AEs between G4 and the experimental values are less pronounced because of the transition barriers for the fragmentation processes. The high barriers impose experimental difficulty in determining the energetics of  $\text{Si}_2\text{H}_2^+$ ,  $\text{Ge}_2\text{H}_2^+$ , and  $\text{SiGeH}_2^+$  using the measured AEs because of the kinetic shift and small Franck-Condon factors at the dissociation and ionization thresholds.

## Acknowledgments

L.W. thanks for the service of SCUTGrid provided by Information Network Research and Engineering Center of South China University of Technology and financial support from National Science Foundation of China (No. 20777017) and the Fundamental Research Fund for the Central Universities of China (2009ZM0176). J.Z. thanks the financial support from US National Science Foundation (CHE-0848643).

## Appendix A. Supplementary data

Supplementary data associated with this article can be found, in the online version, at [doi:10.1016/j.ijms.2011.12.005](https://doi.org/10.1016/j.ijms.2011.12.005).

## References

- [1] J. Ouellette, *Ind. Phys.* (2002) 22 (June/July).
- [2] M. Isomura, K. Nakahata, M. Shima, S. Taira, K. Wakisaka, M. Tanaka, S. Kiyama, *Solar Energy Mater. Solar Cell.* 74 (2002) 519.
- [3] S. Miyazaki, H. Takahashi, H. Yamashita, M. Narasaki, M. Hirose, *J. Non-Cryst. Solids* 299–302 (2002) 148.
- [4] G. Isella, D. Chrastina, B. Rossner, T. Hackbarth, H.-J. Herzog, U. Konig, H. von Kanel, *Solid-State Electron.* 48 (2004) 1317.
- [5] E. Lopez, S. Chiussi, J. Serra, P. Gonzalez, C. Serra, U. Kosch, B. Leon, F. Fabbri, L. Fornarini, S. Martelli, *Appl. Surf. Sci.* 234 (2004) 422.
- [6] J.J. Zhang, K. Shimizu, J. Hanna, *J. Non-Cryst. Solids* 299–302 (2002) 163.
- [7] J. Olivares, J. Sangrador, A. Rodrihuez, T. Rodriguez, *J. Electrochem. Soc.* 148 (2001) C685.
- [8] C.J. Ritter, C.-W. Hu, A.V.G. Chizmeshya, J. Tolle, D. Klewer, I.S.T. Tsong, J. Kouvetakis, *J. Am. Chem. Soc.* 127 (2005) 9855.
- [9] S. Sivaram, *Chemical Vapor Deposition: Thermal and Plasma Deposition of Electronic Materials*, International Thomson Publishing Inc., New York, 1995.
- [10] S.R. Gunn, J.H. Kindsvater, *J. Phys. Chem.* 70 (1966) 1750.

- [11] F.E. Saalfeld, H.J. Svec, *J. Phys. Chem.* 70 (1966) 1753.
- [12] J. Drowart, G.D. Maria, A.J.H. Boerboom, M.G. Inghram, *J. Chem. Phys.* 30 (1959) 308.
- [13] R. Viswanathan, R.W. Schmude, K.A. Gingerich Jr., *J. Chem. Thermodyn.* 27 (1995) 763.
- [14] J. Andzelm, N. Russo, D.R. Salahub, *J. Chem. Phys.* 87 (1987) 6562.
- [15] S.-D. Li, Z.-G. Zhao, X.-F. Zhao, H.-S. Wu, Z.-H. Jin, *Phys. Rev. B* 64 (2001) 195312.
- [16] L. Sari, Y. Yamaguchi, H.F. Schaefer, *J. Chem. Phys.* 119 (2003) 8266.
- [17] P. Wielgus, S. Roszak, D. Majumdar, J. Saloni, J. Leszczynski, *J. Chem. Phys.* 128 (2008) 144305.
- [18] C. Weng, J. Kouvetakis, A.V.G. Chizmeshya, *J. Comput. Chem.* 32 (2011) 835.
- [19] P. Ho, M.E. Coltrin, J.S. Binkley, C.F. Melius, *J. Phys. Chem.* 90 (1986) 3399.
- [20] A.F. Sax, J. Kalcher, *J. Phys. Chem.* 95 (1991) 1768.
- [21] L.A. Curtiss, K. Raghavachari, P.W. Deutsch, J.A. Pople, *J. Chem. Phys.* 95 (1991) 2433.
- [22] G. Katzer, M.C. Ernst, A.F. Sax, J. Kalcher, *J. Phys. Chem. A* 101 (1997) 3942.
- [23] M.T. Swihart, S.L. Girshick, *J. Phys. Chem. B* 103 (1999) 64.
- [24] H.-W. Wong, J.C.A. Nieto, M.T. Swihart, L.J. Broadbelt, *J. Phys. Chem. A* 108 (2004) 874.
- [25] A. Ricca, C.W. Bauschlicher Jr., *J. Phys. Chem. A* 103 (1999) 11121.
- [26] R.S. Grev, H.F. Schaefer, K.M. Baines III, *J. Am. Chem. Soc.* 112 (1990) 9458.
- [27] T.L. Windus, M.S. Gordon, *J. Am. Chem. Soc.* 114 (1992) 9559.
- [28] R.S. Grev, H.F. Schaefer III, *Organometallics* 11 (1992) 3489.
- [29] H. Jacobson, T. Ziegler, *J. Am. Chem. Soc.* 116 (1994) 3667.
- [30] A.J. Boone, D.H. Magers, J. Leszczynski, *Int. J. Quantum Chem.* 70 (1998) 925.
- [31] J.M. Galbraith, H.F. Schaefer III, *J. Mol. Struct. (Theochem)* 424 (1998) 7.
- [32] L. Sari, M.C. McCarthy, H.F. Schaefer III, P. Thaddeus, *J. Am. Chem. Soc.* 125 (2003) 11409.
- [33] R.S. Grev, H.F. Schaefer III, *J. Chem. Phys.* 97 (1992) 7990.
- [34] C. Liang, L.C. Allen, *J. Am. Chem. Soc.* 112 (1990) 1039.
- [35] G. Trinquier, J.P. Malrieu, *J. Am. Chem. Soc.* 109 (1987) 5303.
- [36] Y. Yamaguchi, B.H. DeLeeuw, C.A. Richards, H.F. Schaefer Jr., G. Frenking III, *J. Am. Chem. Soc.* 116 (1994) 11922.
- [37] G. Trinquier, J.-P. Malrieu, P. Riviere, *J. Am. Chem. Soc.* 104 (1982) 4529.
- [38] S. Nagase, T. Kudo, *Theochem* 12 (1983) 35.
- [39] R.S. Grev, B.J. DeLeeuw, H.F. Schaefer III, *Chem. Phys. Lett.* 165 (1990) 257.
- [40] G. Trinquier, *J. Am. Chem. Soc.* 112 (1990) 2130.
- [41] Z. Palagyi, H.F. Schaefer, E. Kapuy III, *J. Am. Chem. Soc.* 115 (1993) 6901.
- [42] H.-J. Himmel, H. Schnockel, *Chem. Eur. J.* 8 (2002) 2397.
- [43] M.J. Frisch, G.W. Trucks, H.B. Schlegel, G.E. Scuseria, M.A. Robb, J.R. Cheeseman, J.A. Montgomery, T. Vreven, K.N. Kudin, J.C. Burant, J.M. Millam, S.S. Iyengar, J. Tomasi, V. Barone, B. Mennucci, M. Cossi, G. Scalmani, N. Rega, G.A. Petersson, H. Nakatsuji, M. Hada, M. Ehara, K. Toyota, R. Fukuda, J. Hasegawa, M. Ishida, T. Nakajima, Y. Honda, O. Kitao, H. Nakai, M. Klene, X. Li, J.E. Knox, H.P. Hratchian, J.B. Cross, V. Bakken, C. Adamo, J. Jaramillo, R. Gomperts, R.E. Stratmann, O. Yazyev, A.J. Austin, R. Cammi, C. Pomelli, J.W. Ochterski, P.Y. Ayala, K. Morokuma, G.A. Voth, P. Salvador, J.J. Dannenberg, V.G. Zakrzewski, S. Dapprich, A.D. Daniels, M.C. Strain, O. Farkas, D.K. Malick, A.D. Rabuck, K. Raghavachari, J.B. Foresman, J.V. Ortiz, Q. Cui, A.G. Baboul, S. Clifford, J. Cioslowski, B.B. Stefanov, G. Liu, A. Liashenko, P. Piskorz, I. Komaromi, R.L. Martin, D.J. Fox, T. Keith, M.A. Al-Laham, C.Y. Peng, A. Nanayakkara, M. Challacombe, P.M.W. Gill, B. Johnson, W. Chen, M.W. Wong, C. Gonzalez, J.A. Pople, *Gaussian 03*, Wallingford, CT, 2004.

- [44] B. Chan, J. Deng, L. Radom, *J. Chem. Theory Comput.* 7 (2011) 112.
- [45] J.P. Merrick, D. Moran, L. Radom, *J. Phys. Chem. A* 111 (2007) 11683.
- [46] L.A. Curtiss, P.C. Redfern, K. Raghavachari, *J. Chem. Phys.* 126 (2007) 084108.
- [47] H. Oberhammer, T. Lobreyer, W. Sundermeyer, *J. Mol. Struct.* 323 (1994) 125.
- [48] G. Dolgonos, *Chem. Phys. Lett.* 454 (2008) 190.
- [49] G. Dolgonos, *Chem. Phys. Lett.* 466 (2008) 11.
- [50] D. Sillars, C.J. Bennett, Y. Osamura, R.I. Kaiser, *Chem. Phys. Lett.* 392 (2004) 541.
- [51] E. Aprà, T.L. Windus, T.P. Straatsma, E.J. Bylaska, W.A. de Jong, S. Hirata, M. Valiev, M. Hackler, L. Pollack, K. Kowalski, R. Harrison, M. Dupuis, D.M.A. Smith, J. Nieplocha, V. Tipparaju, M. Krishnan, A.A. Auer, E. Brown, G. Cisneros, G.I. Fann, H. Fruchtl, J. Garza, K. Hirao, R. Kendall, J.A. Nichols, K. Tsemekhman, K. Wolinski, J. Anchell, D. Bernholdt, P. Borowski, T. Clark, D. Clerc, H. Dachsel, M. Deegan, K. Dyall, D. Elwood, E. Glendening, M. Gutowski, A. Hess, J. Jaffe, B. Johnson, J. Ju, R. Kobayashi, R. Kutteh, Z. Lin, R. Littlefield, X. Long, B. Meng, T. Nakajima, S. Niu, M. Rosing, G. Sandrone, M. Stave, H. Taylor, G. Thomas, J. Van Lenthe, A. Wong, Z. Zhang, NWChem, A Computational Chemistry Package for Parallel Computers, Version 4.7, Pacific Northwest National Laboratory, Richland, WA 99352-0999, USA, 2005.
- [52] B. Ruscic, J. Berkowitz, *J. Chem. Phys.* 95 (1991) 2416.
- [53] B. Ruscic, J. Berkowitz, *J. Chem. Phys.* 95 (1991) 2407.
- [54] L.T. Ueno, L.R. Marim, A.T. Dal Pino, F.B.C. Machado, *Int. J. Quantum Chem.* 106 (2006) 2677.
- [55] P.W. Deutsch, L.A. Curtiss, J.P. Blaudeau, *Chem. Phys. Lett.* 270 (1997) 413.
- [56] K. Fuke, S. Yoshida, *Eur. Phys. J. D* 9 (1999) 123.
- [57] S.-D. Li, Z.-G. Zhao, H.-S. Wu, Z.-H. Jin, *J. Chem. Phys.* 115 (2001) 9255.
- [58] I. Shim, M. Sai Baba, K.A. Gingerich, *Chem. Phys.* 277 (2002) 9.
- [59] A.E. Reed, L.A. Curtiss, F. Weinhold, *Chem. Rev.* 88 (1988) 899.
- [60] J. Berkowitz, G.B. Ellison, D. Gutman, *J. Phys. Chem.* 98 (1994) 2744.
- [61] A. Marijnissen, J.J. ter Meulen, *Chem. Phys. Lett.* 263 (1996) 803.
- [62] D.A. Dixon, D. Feller, K.A. Peterson, J.L. Gole, *J. Phys. Chem. A* 104 (2000) 2326.